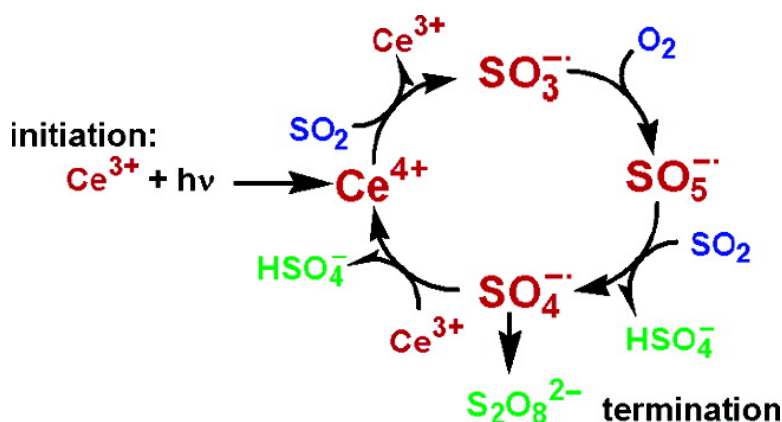


Highly Efficient Photoinitiation in the Cerium(III)-Catalyzed Aqueous Autoxidation of Sulfur(IV). An Example of Comprehensive Evaluation of Photoinduced Chain Reactions

Ildik Kerezsi, Gbor Lente, and István F. Bin

J. Am. Chem. Soc., **2005**, 127 (13), 4785-4793 • DOI: 10.1021/ja0439120 • Publication Date (Web): 10 March 2005

Downloaded from <http://pubs.acs.org> on March 25, 2009



More About This Article

Additional resources and features associated with this article are available within the HTML version:

- Supporting Information
- Links to the 4 articles that cite this article, as of the time of this article download
- Access to high resolution figures
- Links to articles and content related to this article
- Copyright permission to reproduce figures and/or text from this article

[View the Full Text HTML](#)



ACS Publications
 High quality. High impact.

Highly Efficient Photoinitiation in the Cerium(III)-Catalyzed Aqueous Autoxidation of Sulfur(IV). An Example of Comprehensive Evaluation of Photoinduced Chain Reactions

Ildikó Kerecsi, Gábor Lente, and István Fábián*

Contribution from the University of Debrecen, Department of Inorganic and Analytical Chemistry, Debrecen 10, P.O.B. 21, H-4010, Hungary

Received October 6, 2004; E-mail: ifabian@delfin.unideb.hu

Abstract: The photoinitiated and cerium(III)-catalyzed aqueous reaction between sulfite ion and oxygen has been studied in a diode-array spectrophotometer using the same light beam for excitation and detection. Cerium(III) is identified as the photoactive absorbing species, and the production of cerium(IV) initiates a radical chain reaction. To interpret all the experimental findings, a simple scheme is proposed, in which the additional chain carriers are sulfite ion radical ($\text{SO}_3^{\cdot-}$), sulfate ion radical ($\text{SO}_4^{\cdot-}$), and peroxomonosulfate ion radical ($\text{SO}_5^{\cdot-}$). The overall rate of oxidation is proportional to the square root of the light intensity per unit volume, which is readily interpreted by the second-order termination reaction of the proposed scheme. It is also shown that the reaction proceeds for an extended period of time in the dark following illumination, and a quantitative analysis is presented for this phase as well. The postulated model predicts that cerium(III) should have a cocatalytic or synergistic effect on the autoxidation of sulfite ion in the presence of other catalysts. This prediction was confirmed in the iron(III)–sulfite ion–oxygen system. The experimental method and the mathematical treatment used might be applicable to a wide range of photoinduced chain reactions.

Introduction

Catalytic autoxidation of sulfur(IV)¹ has attracted considerable interest because of its dominant role in acid rain formation and importance in industrial desulfurization processes.^{2–6} The sulfite ion–oxygen system has been used for hydroxylation, epoxidation, and oxidative cleavage of DNA.^{7–9} The autoxidation of sulfite ion is also important in metallurgical technologies^{10,11} and food chemistry.^{12,13} Multivalent metal ions are known to be very active catalysts of this reaction, and stoichiometric, kinetic, and mechanistic aspects of several systems have been studied intensively since the 1930s.^{2–38} Bäckström postulated that the formation of transition metal sulfite complexes and their

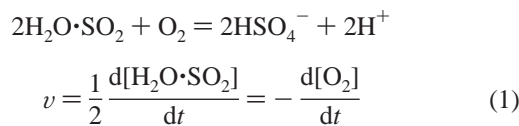
decomposition are mainly responsible for the catalytic effect.¹⁴ Since then, it has been shown that the sulfite complexes may either trigger a radical-type chain reaction by generating the $\text{SO}_3^{\cdot-}$ radical or be part of a direct oxidation of sulfite ion to sulfate ion. All of the postulated mechanisms share the same feature that oxygen is involved only in secondary reaction steps in the overall process.

While many of the metal-ion-catalyzed systems are reasonably well understood now, gaining further mechanistic information on the core autoxidation is often circuitous. First of all, the concentration of dissolved oxygen cannot be controlled as accurately as that of other reactants. The second problem is that while spectroscopic observations are typically suitable for monitoring the metal catalysts or the sulfite complexes, direct information on the concentrations of oxygen or free sulfite ion is not acquirable. Finally, the complexation of the catalyst with sulfite ion is kinetically coupled with the autoxidation process, and very often redox reactions also occur in the absence of oxygen; e.g., the iron(III) complexes are probably the most frequently used catalysts of the autoxidation, but they also oxidize sulfite ion.^{17–18,22,30,37–38}

- (1) Throughout this work, we use the term “sulfite ion” in a general sense to refer collectively to SO_3^{2-} and all of its singly or doubly protonated forms. Differentiation between these forms in the text is only made when it is particularly important for clarity. As no evidence for the existence of sulfurous acid, H_2SO_3 , is known, we adopt the notation $\text{H}_2\text{O}\cdot\text{SO}_2$ for hydrated sulfur dioxide emphasizing that it is the doubly protonated conjugate acid form of SO_3^{2-} .
- (2) Coichev, N.; van Eldik, R. *J. Chem. Educ.* **1994**, *71*, 767.
- (3) Brandt, C.; van Eldik, R. *Chem. Rev.* **1995**, *95*, 119 and references therein.
- (4) Moya, H. D.; Neves, E. A.; Coichev, N. *J. Chem. Educ.* **1999**, *76*, 930.
- (5) Pezza, H. R.; Lopes, C. F. F.; Suárez-Iba, M. E. V.; Coichev, N. *Quim. Nova* **1999**, *22*, 529.
- (6) Csordás, V.; Fábián, I. *Adv. Inorg. Chem.* **2003**, *54*, 395.
- (7) Muller, J. G.; Hickerson, R. P.; Perez, R. J.; Burrows, C. J. *J. Am. Chem. Soc.* **1997**, *119*, 1501.
- (8) Lepentisiotis, V.; Domagala, J.; Grgić, I.; van Eldik, R.; Muller, J. G.; Burrows, C. J. *Inorg. Chem.* **1999**, *38*, 3500.
- (9) Wietzerbin, K.; Muller, J. G.; Jameton, R. A.; Pratiel, G.; Bernadou, J.; Meunier, B.; Burrows, C. J. *Inorg. Chem.* **1999**, *38*, 4123.
- (10) Tiwari, B. L.; Kolbe, J.; Hayden, H. W., Jr. *Metall. Trans. B* **1979**, *10*, 607.
- (11) Cho, E. H. *Metall. Trans. B* **1986**, *17*, 745.
- (12) Wedziha, B. L.; Lamikanra, O. *Food Chem.* **1987**, *23*, 193.
- (13) McFeeters, R. F.; Barrangou, L. M.; Barish, A. O.; Morrison, S. S. *J. Agric. Food Chem.* **2004**, *52*, 4554.

- (14) Bäckström, H. L. *J. Z. Phys. Chem., Abt. B* **1934**, *25*, 122.
- (15) Anast, J. M.; Margerum, D. W. *Inorg. Chem.* **1981**, *20*, 2319.
- (16) Hobson, D. B.; Richardson, P. J.; Robinson, P. J.; Hewitt, E. A.; Smith, I. *Ind. Eng. Chem. Res.* **1987**, *26*, 1818.
- (17) Kraft, J.; van Eldik, R. *Atmos. Environ.* **1989**, *23*, 2709.
- (18) Kraft, J.; van Eldik, R. *J. Chem. Soc., Chem. Commun.* **1989**, 790.
- (19) van Eldik, R.; Coichev, N.; Bal Reddy, K.; Gerhard, A. *Ber. Bunsen-Ges. Phys. Chem.* **1992**, *96*, 478.
- (20) Timpe, O.; Schlögl, R. *Ber. Bunsen-Ges. Phys. Chem.* **1993**, *97*, 1076.
- (21) Berglund, J.; Fronaeus, S.; Elding, L. I. *Inorg. Chem.* **1993**, *32*, 4527.
- (22) Brandt, C.; Fábián, I.; van Eldik, R. *Inorg. Chem.* **1994**, *33*, 687 and references therein.

In this paper, we describe an exceptional case where the mechanism of the photoinitiated and Ce^{3+} -catalyzed autoxidation of sulfite ion could be explored in detail. Equation 1 defines the stoichiometry and the rate of the overall process:



This system offers several unique advantages, making it possible to draw unambiguous conclusions regarding the mechanism. First of all, complex formation or direct redox reactions do not occur between Ce^{3+} and sulfite ions, and consequently there is no interference from such processes. Second, the concentration change of sulfite ion can be followed directly by UV–vis spectroscopy. Third, the autoxidation is zeroth-order with respect to dissolved oxygen, circumventing the problem of less accurate control over its concentration. Fourth, due to the photoinitiated nature of the reaction, it can be started and ceased by turning illumination on and off, respectively.

A further point of interest in the present study is the widespread analytical use of the Ce^{4+} –sulfite ion reaction.^{39–41} Although quite a few methods have been developed based on this process, no attention has been directed toward possible interference from dissolved oxygen or light. Further on, in a few cases the interpretation of the chemical principles of the analysis is clearly incoherent and without ground.

Experimental Section

Materials. All chemicals used in this study were of analytical reagent grade and purchased from commercial sources. $\text{CeCl}_3\cdot 6\text{H}_2\text{O}$ (Aldrich) and $\text{Ce}(\text{SO}_4)_2\cdot 4\text{H}_2\text{O}$ (Reanal) were used without further purification to prepare stock solutions. The concentration of the Ce^{3+} stock solution was determined by complexometric titration with Na_2EDTA solution at pH between 5 and 6 using xylenolorange indicator. The concentration of the Ce^{4+} stock solution was determined by iodometric titration. Fresh sodium sulfite stock solutions were prepared from $\text{Na}_2\text{S}_2\text{O}_5$ (Reanal) every day. Doubly deionized and ultrafiltered water from a Millipore Q system was used to prepare the stock solutions and samples. All experiments were carried out at high and constant acid concentration (sulfuric or perchloric acid), and additional salt was not used to adjust the ionic strength.

Instrumentation. UV–vis spectra were recorded on a HP-8543 diode-array or a Perkin-Elmer Lambda 2S scanning spectrophotometer. A YSI 5100 dissolved oxygen meter and a YSI model 5239 probe with YSI 5906 membrane cap were used for measuring the concentration of dissolved oxygen in aqueous solutions. Two different lamps were used in some of the photochemical experiments: an AvaLight DHS (Avantes) and a high-power quartz lamp (Medicor, Hungary). Quantitative kinetic measurements on the photochemical reaction were performed on the HP-8543 diode-array instrument using the method and general operating procedures described in an earlier publication.⁴² A built-in Hewlett-Packard 89090A Peltier thermostat was used to maintain constant temperature (10.0 ± 0.1 or 25.0 ± 0.1 °C). The solutions were kept homogeneous during the photochemical experiments using the built-in magnetic stirrer of the standard cell compartment of the HP-8543 instrument. A 3-mm stirring rod was used inside standard quartz cuvettes (optical path length: 1.000 cm). The geometry of the setup was carefully tested, and it was made sure that the stirring rod never disrupted the light beam. The light source was calibrated by both ferrioxalate actinometry⁴³ and reproducing observations on the known photoreaction of 2,6-dichloro-1,4-benzoquinone.⁴² Some additional kinetic measurements on thermal reactions were performed with an Applied Photophysics DX-17 MV sequential stopped-flow apparatus using a 1 cm optical path length.

Results and Discussion

Preliminary Observations. Sulfite ion and oxygen do not react in the absence of catalysts in acidic aqueous solutions, even at elevated temperatures.^{3,5,36,44} We confirmed that Ce^{3+} has a catalytic effect on reaction 1 in our earlier high-temperature study on the effect of dissolved oxygen on the aqueous redox reactions of dithionate ion.⁴⁴ This phenomenon was rather unexpected, as the only previous related record known to us is a remark about possible effect of Ce^{4+} on the autoxidation of sulfite ion in a study connected to seawater chemistry.¹⁶ We found that the catalytic process can be studied in a straightforward manner at room temperature.

In preliminary studies on the Ce^{3+} –sulfite ion–oxygen system, the same experiments were carried out in a conventional double beam and a HP-8453 diode-array spectrophotometer. Measurable progress of sulfite ion decay was observed only with the latter instrument. The main difference in the experiments is that the double-beam unit scans the spectrum with a low intensity monochromatic light beam, whereas the diode-array spectrophotometer irradiates the sample with a relatively high energy undispersed light in the 190–1100 nm spectral region. The observations confirm that illumination of the samples with sufficient light intensity is essential in the $\text{Ce}(\text{III})$ -catalyzed autoxidation of sulfite ion and the reaction can be driven even by the light source of a standard photometer.

The photochemical nature of the process is demonstrated in Figure 1. In this case, the variation in the concentration of dissolved oxygen was followed in a solution containing sulfite ion and Ce^{3+} . A steady decay in the oxygen concentration was observed as long as the light source of a commercially available Avantes fiber optic spectrophotometer was illuminating the solution. When the light source was turned off, the concentration change was reversed. The experiment was run in an open reactor, and thus the slight increase in the concentration occurred because of the dissolution of oxygen from ambient air. Similar

- (23) Berglund, J.; Elding, L. I. *Atmos. Environ.* **1995**, *29*, 1379.
 (24) Connick, R. E.; Zhang, Y. X. *Inorg. Chem.* **1996**, *35*, 4613.
 (25) Ermakov, A. N.; Proskrebyshev, G. A.; Stoliarov, S. I. *J. Phys. Chem.* **1996**, *100*, 3557.
 (26) Ermakov, A. N.; Proskrebyshev, G. A.; Purmal, A. P. *Kinet. Catal.* **1997**, *38*, 325.
 (27) Travina, O. A.; Kozlov, Y. N.; Purmal, A. P.; Travina, S. O. *Kinet. Catal.* **1997**, *38*, 242.
 (28) Fronaeus, S.; Berglund, J.; Elding, L. I. *Inorg. Chem.* **1998**, *37*, 4939.
 (29) Grgić, I.; Dovžan, A.; Berčič, G.; Hudnik, V. J. *Atmos. Chem.* **1998**, *29*, 315.
 (30) Brandt, C.; van Eldik, R. *Transition Met. Chem.* **1998**, *23*, 667.
 (31) Grgić, I.; Poznić, M.; Bizjak, M. *J. Atmos. Chem.* **1999**, *33*, 89.
 (32) Pezza, H. R.; Coichev, N. J. *Coord. Chem.* **1999**, *47*, 107.
 (33) Martins, C. R.; Cabral Neto, C. A.; Alves, J. J. F.; Andrade, J. B. *J. Braz. Chem. Soc.* **1999**, *10*, 453.
 (34) Wolf, A.; Deutsch, F.; Hoffmann, P.; Ortner, H. M. *J. Atmos. Chem.* **2000**, *37*, 125.
 (35) Betterton, E. A.; Anderson, D. J. *J. Atmos. Chem.* **2001**, *40*, 171.
 (36) Ermakov, A. N.; Purmal, A. P. *Kinet. Catal.* **2001**, *42*, 479.
 (37) Lente, G. Ph.D. Thesis, University of Debrecen, Hungary, 2001. Available free of charge via the Internet at <http://www.unideb.hu/~lenteg/index.html>
 (38) Lente, G.; Fábán, I. *J. Chem. Soc., Dalton Trans.* **2002**, 778.
 (39) Takeuchi, K.; Ibusuki, T. *Anal. Chim. Acta* **1985**, *174*, 359.
 (40) Koukili, I. I.; Sarantonis, E. G.; Calokerinos, A. C. *Anal. Lett.* **1990**, *23*, 1167.
 (41) Aly, F. A.; Alarfaj, N. A.; Alwarthan, A. A. *Talanta* **2001**, *52*, 715.

- (42) Lente, G.; Espenson, J. H. *J. Photochem. Photobiol., A* **2004**, *163*, 249.
 (43) Hatchard, C. G.; Parker, C. A. *Proc. R. Soc. London, Ser. A* **1956**, *235*, 518.
 (44) Lente, G.; Fábán, I. *Inorg. Chem.* **2004**, *43*, 4019.

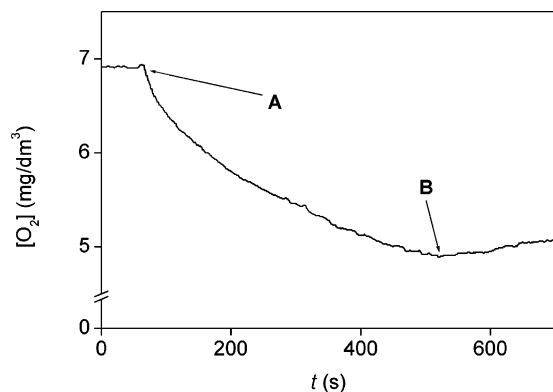


Figure 1. Effect of light on the dissolved oxygen concentration in the presence of sulfite ion and Ce^{3+} . (A) Start of illumination. (B) End of illumination. $[\text{Ce}^{3+}] = 0.50 \text{ mM}$; $[\text{S(IV)}] = 1.00 \text{ mM}$; $[\text{H}_2\text{SO}_4] = 0.10 \text{ M}$; $T = 25 \text{ }^\circ\text{C}$.

effects were not observed in the absence of either Ce^{3+} or sulfite ion. The same conclusions were drawn when a quartz lamp was used instead of the less intense light beam of the spectrophotometer (Figure S1 in Supporting Information). The loss of oxygen was so rapid in this case that reliable kinetic measurements were not possible because of the relatively slow response time of the oxygen electrode.⁴⁵

Stoichiometric studies were also carried out. The dissolved oxygen content of a freshly prepared acidic solution containing Ce^{3+} and sulfite ion was measured, and then the quartz lamp was used to drive the reaction until the concentration of dissolved oxygen dropped to zero. The sulfite concentration of this sample was determined by measuring its UV–vis spectrum immediately. It should be noted that $\text{H}_2\text{O}\cdot\text{SO}_2$ is the predominant form of sulfite ion in the entire pH range of the present study ($\text{p}K_{\text{a}1} = 1.74$ at $25.0 \text{ }^\circ\text{C}$ in 1.0 M NaClO_4) and it has a UV absorption band centered around 276 nm .^{37,38} These studies showed that the stoichiometry of the reaction corresponds to eq 1 within experimental error.

When the photoinitiation is carried out in the diode-array spectrophotometer, the spectrum of the solution can be recorded simultaneously. A recently introduced method uses the same light beam to drive and analyze the photochemical reaction.⁴² This technique has remarkable potential for extending quantitative kinetic measurements on photochemical reactions. Typical kinetic traces measured in the Ce^{3+} –sulfite ion system at 276 nm are shown in Figure 2. These experiments afforded quantitative information about the process and will be discussed in detail in the next sections.

Identification of the Photoactive Species. Only UV light is absorbed by the components of the Ce(III)–sulfite ion system because $\text{H}_2\text{O}\cdot\text{SO}_2$ and Ce^{3+} have absorptions in the $195\text{--}300 \text{ nm}$ range (Figure S2 in Supporting Information). An analysis of the spectra recorded during the kinetic experiments proved that no detectable amounts of Ce^{4+} , which has strong absorption at around 320 nm ,⁴⁴ formed during the reaction at any time.

Under the conditions of the kinetic studies, both $\text{H}_2\text{O}\cdot\text{SO}_2$ and Ce^{3+} contribute significantly to the overall absorbance, although the relative values are different at different wavelengths. Consequently, both of them can in principle be photoactive species. Based on the measurements carried out in

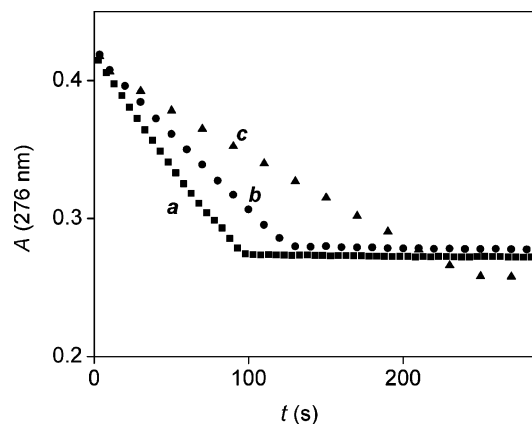


Figure 2. Kinetic traces measured in a diode-array instrument during the photoinitiated autoxidation of sulfite ion. $[\text{Ce}^{3+}] = 0.50 \text{ mM}$; $[\text{S(IV)}] = 1.00 \text{ mM}$; $[\text{O}_2] = 0.19 \text{ mM}$ (a, b), 0.22 mM (c); $[\text{H}_2\text{SO}_4] = 0.10 \text{ M}$; path length 1.000 cm ; $V = 3.00 \text{ cm}^3$; $T = 25.0 \text{ }^\circ\text{C}$; $t_i = 5 \text{ s}$; $t_d = 0 \text{ s}$ (a), 5 s (b), 15 s (c); $\lambda = 276 \text{ nm}$.

the sulfite ion–oxygen– Ce^{3+} system, we found no obvious way to decide which reactant is the photoactive species.

However, an experiment reported in our earlier study on the oxidation of dithionate ion conclusively shows that Ce^{3+} is the active absorbing species.⁴⁴ In this experiment (shown in Figure 5 in ref 39 and in Figure S3 in the Supporting Information), the slow disproportionation of dithionate ion produced sulfite ion, which was in turn oxidized by dissolved oxygen in a Ce(III)-catalyzed process. The observed kinetic curves and repetitive spectra showed that no sulfite ion accumulated in any detectable concentration until all oxygen was consumed. During the whole course of this reaction, Ce^{3+} is the only absorbing species present; therefore light absorption by sulfite ion is not necessary for driving the reaction, and Ce^{3+} must be the photoactive species. As will be shown in the next sections, this conclusion is also consistent with the results obtained here because quantitative evaluation of all kinetic observations is possible assuming that Ce^{3+} is the only photoactive reactant.

Experiments with Continuous Illumination. Photochemical kinetic experiments can be performed with a diode-array spectrophotometer in different ways. Essentially, the variants differ in the illumination time of the sample during the measurement of a single spectrum and in the duration of dark periods between recording two consecutive spectra, when the illuminating light is excluded by closing the shutter of the photometer. The lengths of the illumination and dark periods are given by t_i and t_d , respectively. Thus, the duration of a full cycle, t_c , is given by $t_c = t_i + t_d$. The simplest experiment is when the sample is continuously illuminated after triggering the reaction, i.e., $t_d = 0$. Typical kinetic traces recorded using this concept are shown in Figure 2. The reaction becomes slower by increasing the length of the dark periods because the same amount of light illuminates the sample over a longer period of time. However, the rate does not decrease proportionally to the cycle time. This clearly indicates that thermal reactions during the dark periods also contribute to the overall process.

The photochemical use of diode-array instruments also affords a way to determine quantum yields after careful calibration.⁴² The quantum yield of oxygen loss relative to the number of photons absorbed by Ce^{3+} in the fastest experiment shown in Figure 2 (with $t_d = 0 \text{ s}$) was determined to be 76 ± 6 . This unequivocally indicates some kind of chain mechanism in which

(45) Maccà, C. *Anal. Chim. Acta* **2004**, *512*, 183.

the role of light is only to initiate the chain but not to maintain its propagation. In addition, the detected kinetic traces and rates were also dependent on temperature (Figure S4 in Supporting Information) indicating that the overall process involves thermal reactions before or in the rate-determining step.

As shown in Figure 2, the measured kinetic traces are straight lines; i.e., the rate did not depend on the time elapsed within a kinetic run. The ratio of the initial concentrations of sulfite ion and oxygen was reasonably close to the stoichiometric 2:1, so one can conclude that the reaction is zeroth-order with respect to both dissolved oxygen and sulfite ion. The same conclusion was drawn from experiments with different initial concentrations of the reactants. At 276 nm, the molar absorbances of $\text{H}_2\text{O}\cdot\text{SO}_2$ and Ce^{3+} were measured in independent experiments (Figure S2 in Supporting Information). The concentration of Ce^{3+} does not change during the process, so the decrease in absorbance is entirely due to the loss of $\text{H}_2\text{O}\cdot\text{SO}_2$. Consequently, the rates of absorbance change could readily be converted into the rate of reaction 1 by using the molar absorbance of $\text{H}_2\text{O}\cdot\text{SO}_2$ ($364 \text{ M}^{-1} \text{ cm}^{-1}$) and considering the stoichiometry.

As already pointed out, v did not depend on the concentrations of sulfite ion or oxygen and it was also independent of the ionic strength and the pH in the studied region 0.1–1.0 (Figure S5 in Supporting Information). However, the rate depended on the intensity of light and the concentration of the photoinitiator Ce^{3+} .

The intensity of the driving light cannot be changed directly as the diode-array spectrophotometer has a fixed and carefully stabilized light source. However, it is well-known that the rate of a photochemical reaction is proportional to the intensity of absorbed light per unit volume.⁴⁶ Perhaps, the most convenient way is to use the closely related quantity of absorbed photon count per unit volume in the evaluation of the results,⁴² which is basically the part of the photon flow of the light beam (i.e. number of photons) absorbed by the photoactive species.⁴⁷ The absorbed photon count per unit volume (N_V) can be calculated from the known absorption spectra and concentrations of the components and the emission properties of the carefully calibrated light source⁴² and can be changed readily by varying the volume of the sample irradiated. In the restricted space of a 1 cm standard cuvette the accessible working volume range is fairly limited, but a change by a factor of about 2 can still be achieved, which is suitable for drawing basic conclusions. The results are shown in Figure 3, where the logarithm of the rate is plotted against the logarithm of sample volume. The points define a straight line with some scatter, and the slope is -0.49 ± 0.06 . Thus, the reaction is 0.5 order with respect to N_V . This again indicates a chain mechanism and also strongly suggests that the terminating step is second-order with respect to the chain carriers.⁴⁶

In a more general sense, we note that studying the intensity dependence through changing the volume in photochemical reactions is a very advantageous technique when polychromatic light is used as a driving force. If a series of filters were to be used for the same purpose, they would almost surely change the spectral properties of the driving light, whereas changing the volume leaves the spectral distribution of intensities unaltered.

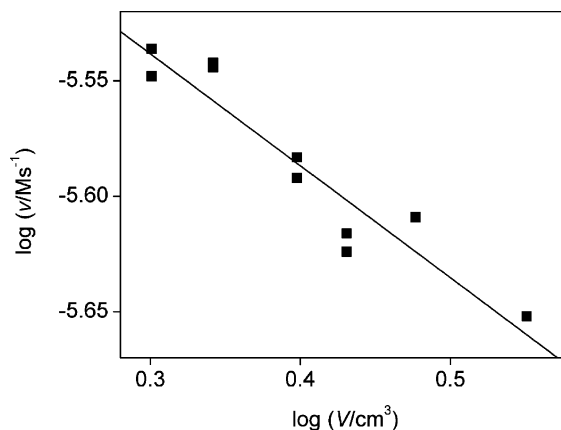


Figure 3. Reaction rates as a function of sample volume. $[\text{Ce}^{3+}] = 0.50 \text{ mM}$; $[\text{S(IV)}] = 1.00 \text{ mM}$; $[\text{H}_2\text{SO}_4] = 0.10 \text{ M}$; $T = 25.0 \text{ }^\circ\text{C}$.

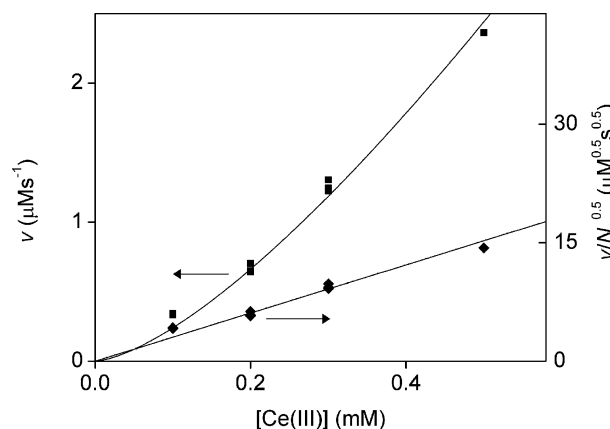


Figure 4. Reaction rates as a function of Ce^{3+} concentration. $[\text{S(IV)}] = 1.00 \text{ mM}$; $[\text{H}_2\text{SO}_4] = 0.10 \text{ M}$; $V = 3.00 \text{ cm}^3$; $T = 25.0 \text{ }^\circ\text{C}$.

The dependence of the reaction rate on the Ce^{3+} concentration is somewhat more complex because N_V itself is dependent on the concentration of Ce^{3+} (kinetic traces are shown in Figure S6 in Supporting Information). A direct plot of v vs $[\text{Ce}^{3+}]$ shows some upward curvature, which is between linear and parabolic (Figure 4, left axis). However, N_V can be calculated for each Ce^{3+} concentration, and the quantity $v/N_V^{0.5}$ shows linear dependence on $[\text{Ce}^{3+}]$ (Figure 4, right axis). This confirms the following overall rate equation:

$$v = k_2[\text{Ce}^{3+}]N_V^{0.5} \quad (2)$$

The value $k_2 = 30 \pm 1 \text{ M}^{-0.5} \text{ s}^{-0.5}$ was determined by multivariate least-squares fitting of all relevant measured data.

Experiments with Intermittent Dark Periods. Measurements were carried out by opening and closing the shutter in the light beam for controlled periods. Detailed experiments were carried out to study the reaction with interrupted illumination under standard conditions ($[\text{Ce}^{3+}] = 0.50 \text{ mM}$; $V = 3.00 \text{ cm}^3$; $T = 25.0 \text{ }^\circ\text{C}$) at which the constant reaction rate upon continuous illumination was $v_0 = (2.3 \pm 0.1) \times 10^{-6} \text{ M s}^{-1}$. As shown by the two slower traces in Figure 2 (the curves with $t_d = 5$ and 15 s), kinetic traces were zeroth-order with interrupted illumination as well.

Because the reaction rate is constant during exposure to light of constant intensity, one would expect that the progress of the reaction is proportional to the time of illumination. As a test, a series of experiments were carried out where t_i and t_c were

(46) Atkins, P. W.; de Paula, J. *Physical Chemistry*, 7th ed.; Oxford University Press: Oxford, 2002; pp 924–936.

(47) Verhoeven, J. W. *Pure Appl. Chem.* **1996**, *68*, 2223.

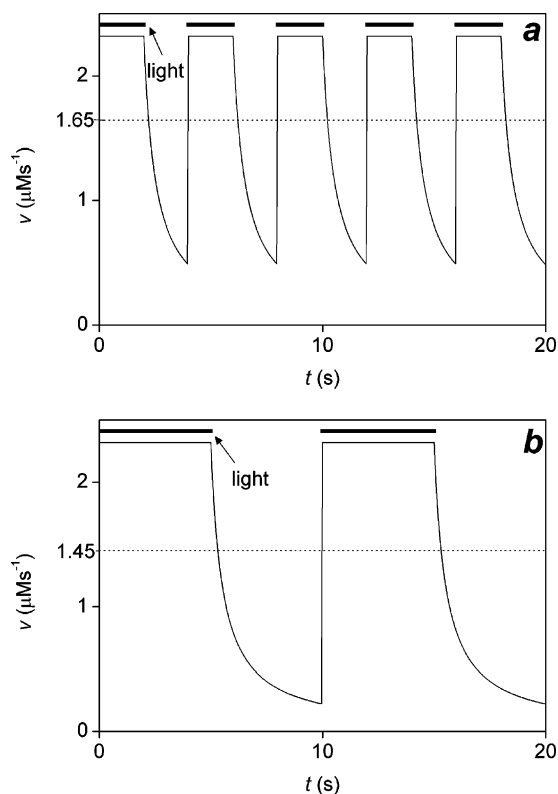


Figure 5. Calculated reaction rate as a function of time during experiments with intermittent dark periods. $[Ce^{3+}] = 0.50$ mM; $[S(IV)] = 1.00$ mM; $[H_2SO_4] = 0.10$ M; $V = 3.00$ cm³; $T = 25.0$ °C; $t_i = t_d = 2$ s (a); $t_i = t_d = 5$ s (b); dotted lines, average rates.

changed simultaneously in such a manner that their ratio was kept constant. In other words, the average amount of photons absorbed during a longer period of reaction time was constant. It would clearly be expected that the average reaction rate measured in such a series of experiments remains unchanged. However, this is not the case, the average reaction rate decreased as t_i increased in this series (Figure S7 in Supporting Information).

Another related unexpected observation was that the quantum yield depended not only on the volume of the samples and the concentration of Ce^{3+} but also on the length and distribution of the dark periods. The highest quantum yield measured in our experiments with long dark periods (t_d) and short illumination times (t_i) exceeded 500. These observations can only be interpreted again by assuming that the reaction persists for some time in the dark periods following illumination.

In fact, the analysis of data (vide infra) showed that the instantaneous reaction rate changes as depicted in the examples of Figure 5, where curve a ($t_i = 2$ s, $t_d = 2$ s) and curve b ($t_i = 5$ s, $t_d = 5$ s) have the same t_i/t_d ratio but exhibit different average rates. At this point, it should be explained why the detected kinetic traces remain zeroth-order despite the varying instantaneous reaction rates in the dark. The reaction remains undetected in the dark period because the spectrophotometer cannot measure without light. The loss of sulfite ion in the dark period is detected during the next illumination phase. Therefore, the difference between two successive observation points is characteristic of the progress of the reaction in a complete cycle (Figure S8 in Supporting Information). The overall progress of the reaction is the same in every cycle, so the detected kinetic trace remains zeroth-order.

This line of reasoning also demonstrates that the average reaction rate v measured in an experiment with interrupted illumination carries information on the progress of the reactions in the dark periods. First, the fraction of the overall reaction occurring in the dark, Q , is defined

$$Q = 1 - \frac{v_0 t_i}{v t_c} \quad (3)$$

Furthermore, the amount of oxygen consumed in the dark period, n , can be calculated as

$$n = v t_c - v_0 t_i \quad (4)$$

Figures 6, 7, and 8 show how Q and n depend on t_i and t_d .

The fact that the reaction still persists somewhat after the end of the illumination is readily interpreted by noting that a chain reaction does not stop immediately after ceasing the initiation. The concentration of the reactive intermediates can only decrease in some time through the termination step(s). Although this time is often very short (10^{-6} – 10^{-3} s) in chain reactions, there is no reason to think that it cannot be longer occasionally.

In general, two fundamentally different chain terminations can be operative.⁴⁶ The termination reaction is first-order with respect to the chain carriers when they react with scavengers being present in relatively large concentrations, while recombination steps yield second-order kinetics.

The instantaneous reaction rate, v_d , as a function of time in the dark period can be given for first-order and second-order termination, respectively:

$$v_d^{1st} = v_0 e^{-k_5 t} \quad (5)$$

$$v_d^{2nd} = \frac{v_0}{1 + k_6 t} \quad (6)$$

In these formulas, v_0 is the rate under illumination, k_5 is a pseudo first-order rate constant, k_6 is the product of a pseudo second-order rate constant and the steady-state concentration of the recombining chain carrier at the end of the illumination period. This concentration is the same for each kinetic run as long as the reactant concentrations and illuminating light intensities are the same.

From eqs 5 and 6, n can readily be calculated by integrating v_d over the time period from 0 to t_d :

$$n^{1st} = \int_0^{t_d} v_d^{1st} dt = \frac{v_0}{k_5} (1 - e^{-k_5 t_d}) \quad (7)$$

$$n^{2nd} = \int_0^{t_d} v_d^{2nd} dt = \frac{v_0}{k_6} \ln(1 + k_6 t_d) \quad (8)$$

From eqs 7 and 8, the value of Q can also be calculated:

$$Q^{1st} = \frac{(1 - e^{-k_5 t_d})}{k_5 t_i + (1 - e^{-k_6 t_d})} \quad (9)$$

$$Q^{2nd} = \frac{\ln(1 + k_6 t_d)}{k_6 t_i + \ln(1 + k_6 t_d)} \quad (10)$$

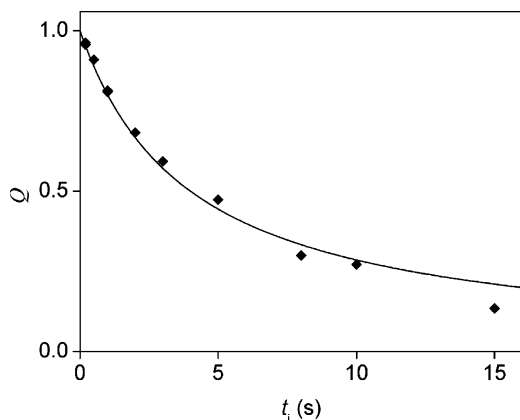


Figure 6. Fraction of the reaction occurring in the dark (Q) as a function of illumination time (t_i) during experiments with intermittent dark periods. Solid line: best fit to eq 9 or 10. $[\text{Ce}^{3+}] = 0.50$ mM; $[\text{S(IV)}] = 1.00$ mM; $[\text{H}_2\text{SO}_4] = 0.10$ M; $V = 3.00$ cm³; $T = 25.0$ °C; $t_d = 90$ s.

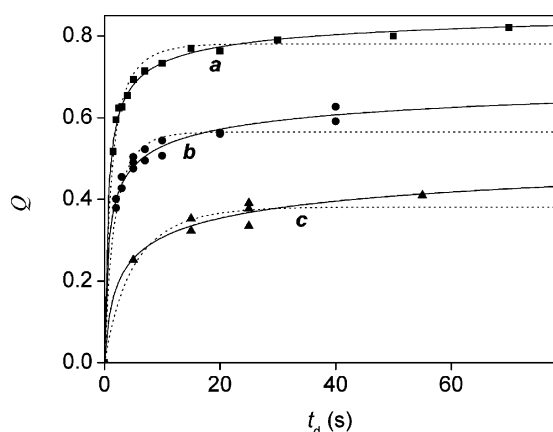


Figure 7. Fraction of the reaction occurring in the dark (Q) as a function of length of the dark periods (t_d) during experiments with intermittent dark periods. Solid line: best fit to the second-order termination model (eq 10). Dotted line: best fit to the first-order termination model (eq 9). $[\text{Ce}^{3+}] = 0.50$ mM; $[\text{S(IV)}] = 1.00$ mM; $[\text{H}_2\text{SO}_4] = 0.10$ M; $V = 3.00$ cm³; $T = 25.0$ °C; $t_i = 1$ s (a), 2 s (b), 5 s (c).

Figure 6 shows the experimental value of Q as a function of t_i with t_d kept constant. Both eqs 9 and 10 fit equally well (solid line) to the measured points in this graph because the equations are parametrically the same if t_d is kept constant. The successful fit confirms the explanation that the thermal reaction proceeds for an extended period of time in the dark because of the relatively slow termination step.

Figure 7 depicts the results from three sets of experiments where t_d was varied at constant t_i ($t_i = 1, 2,$ and 5 s were used). The solid lines represent the best fit to eq 10 (second-order), whereas the dotted lines are the best fits to eq 9 (first-order). The second-order fit is clearly superior to the first-order fit in each case, which suggests that the termination is second-order, in agreement with the conclusion drawn earlier based on the 0.5 order with respect to N_V .

Figure 8 shows how n depends on t_d . Only the second-order fit is shown in the graph. The fit is acceptable, and it is also clear that n is independent of t_i as predicted by eq 8. A numerical analysis of the data set gave $k_6 = 1.9 \pm 0.3$ s⁻¹ for the conditions given.

At this point, it should be noted that the quantitative considerations presented in this section and eqs 3–10 are not dependent on the actual chemistry of the system studied.

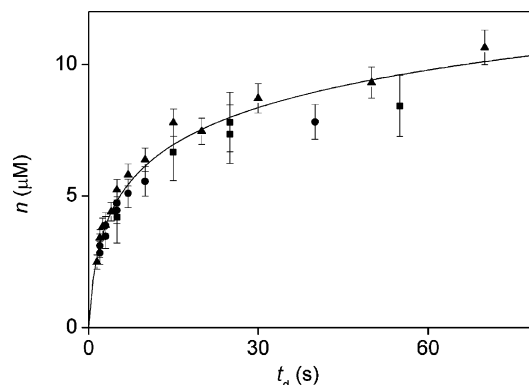
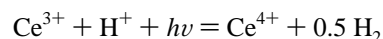


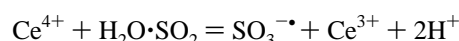
Figure 8. Amount of oxygen consumed in the dark period (n) as a function of length of the dark periods (t_d) during experiments with intermittent dark periods. Solid line: best fit to the second-order termination model (eq 8). $[\text{Ce}^{3+}] = 0.50$ mM; $[\text{S(IV)}] = 1.00$ mM; $[\text{H}_2\text{SO}_4] = 0.10$ M; $V = 3.00$ cm³; $T = 25.0$ °C. Several different integration times shown: $t_i = 5$ s (■), 2 s (●), 1 s (▲).

Therefore the general method and the equations are directly applicable to all photoinitiated chain reactions.

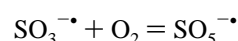
Suggested Mechanism. The autoxidation of sulfite ion is driven by light absorbed by Ce^{3+} , and the corresponding photochemical steps need to be crucial in triggering the overall reaction. Aqueous Ce^{3+} is known to participate in several photochemical processes which produce highly reactive intermediates.⁴⁸ Each of these species is expected to be capable of generating the chain carriers via direct reactions with sulfite ion. First, we postulate a kinetic model with the simplest initiation sequence (eqs 11–16). An alternative model with different initiation steps will be discussed briefly in a subsequent part of the paper.



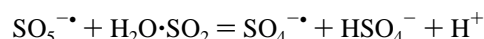
$$v_{11} = \alpha_{11} N_V \quad (11)$$



$$v_{12} = k_{12} [\text{Ce}^{4+}] [\text{H}_2\text{O} \cdot \text{SO}_2] \quad (12)$$



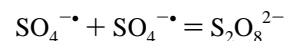
$$v_{13} = k_{13} [\text{SO}_3^{\cdot-}] [\text{O}_2] \quad (13)$$



$$v_{14} = k_{14} [\text{SO}_5^{\cdot-}] [\text{H}_2\text{O} \cdot \text{SO}_2] \quad (14)$$



$$v_{15} = k_{15} [\text{SO}_4^{\cdot-}] [\text{Ce}^{3+}] \quad (15)$$



$$v_{16} = k_{16} [\text{SO}_4^{\cdot-}]^2 \quad (16)$$

It should be noted that α_{11} is fully equivalent to the quantum efficiency of reaction 11,⁴⁷ and k_{12} – k_{16} are second-order rate constants of bimolecular steps.

Photochemical excitation of Ce^{3+} yields Ce^{4+} and hydrogen in aqueous solution. However, the Ce^{4+} formed cannot usually

(48) Shilov, V. P.; Yusov, A. B. *High Energy Chem.* **1999**, *33*, 242 and references therein.

be detected as it oxidizes water and reproduces Ce^{3+} .⁴⁸ This reaction occurs spontaneously even without light, but light accelerates it;⁴⁸ i.e., the net result is photochemical splitting of water in the absence of any other reagents. It is well documented that this process occurs, albeit not particularly efficiently, in aqueous Ce^{3+} solutions upon UV illumination.⁴⁹

The oxidation of water by Ce^{4+} probably becomes inferior compared to other reactions in the presence of a reducing agent such as sulfite ion. In agreement with earlier literature results,⁴⁰ our stopped-flow experiments confirmed that Ce^{4+} oxidizes sulfite ion quite rapidly. The usual time scale of this process is 5–20 ms in 0.1 M H_2SO_4 , and increasing the pH further accelerates the reaction so that it goes to completion within the dead time of the stopped-flow instrument. Thus, Ce^{4+} needs to be present at very low steady-state concentration levels and is considered to be one of the chain carriers. It should be added that competing reactions of Ce^{4+} with other reactants are not feasible in this system.

Cerium(IV) is a typical one-electron oxidant, and as such its reaction with $\text{H}_2\text{O}\cdot\text{SO}_2$ is expected to produce Ce^{3+} and the sulfite ion radical ($\text{SO}_3^{\cdot-}$), which is another chain carrier. The reaction of $\text{SO}_3^{\cdot-}$ with $\text{H}_2\text{O}\cdot\text{SO}_2$ would lead to no net chemical change, and the reaction between $\text{SO}_3^{\cdot-}$ and Ce^{3+} would be the exact reverse of eq 12 and therefore thermodynamically unfavorable. Thus, $\text{SO}_3^{\cdot-}$ is most likely to react only with O_2 (eq 13). This reaction was frequently postulated in elaborated mechanisms for sulfite ion autoxidation.^{3,5,22}

The product of eq 13 is the highly reactive peroxomonosulfate ion radical, $\text{SO}_5^{\cdot-}$, which is a strong oxidant. Its reaction with Ce^{3+} would produce two highly reactive species, Ce^{4+} and the peroxomonosulfate ion SO_5^{2-} , and lead to a branching in the chain. Such an effect (branching in the chain) is clearly not supported by the experimental data, and the oxidation of Ce^{3+} by $\text{SO}_5^{\cdot-}$ was excluded from the kinetic model. An alternative step is the reaction of $\text{SO}_5^{\cdot-}$ with $\text{H}_2\text{O}\cdot\text{SO}_2$ which produces a sulfate ion and a sulfate ion radical ($\text{SO}_4^{\cdot-}$) in a simple oxygen-transfer process. This particular elementary step was also considered in earlier mechanistic studies on the autoxidation of sulfite ion.²² Sulfate ion radical is thus the fourth chain carrier which may either react with $\text{H}_2\text{O}\cdot\text{SO}_2$ or Ce^{3+} to produce $\text{SO}_3^{\cdot-}$ or Ce^{4+} , respectively. The chain would be completed with the formation of both of these two species. However, mathematical analysis showed that the inclusion of the reaction between sulfate ion radical and $\text{H}_2\text{O}\cdot\text{SO}_2$ would clearly predict significant sulfite-ion dependence of the overall rate of the autoxidation. Experimentally no such dependence was observed, and therefore only the reaction of sulfate ion radical with Ce^{3+} is included in the final model. It should be noted that $\text{SO}_4^{\cdot-}$ has a crucial role in the model, because its recombination reaction with another $\text{SO}_4^{\cdot-}$ (eq 16) is assumed to be the termination step.

The rate equation was obtained on the basis of the kinetic model (eqs 11–16) using the long chain approximation.⁵⁰ It should be emphasized that this way of derivation is mathematically equivalent to simply setting steady-state approximations for all of the reactive intermediates in the system, only less tedious algebraically. The main assumption is that the rates of chain carrier formation in initiation and termination should be

equal under steady-state conditions if the chain is reasonably long:

$$\alpha_{11}N_V = 2 \times k_{16}[\text{SO}_4^{\cdot-}]_{\text{ss}}^2 \quad (17)$$

In this equation, $[\text{SO}_4^{\cdot-}]_{\text{ss}}$ is the steady-state concentration of the sulfate ion radical, which can be expressed as follows:

$$[\text{SO}_4^{\cdot-}]_{\text{ss}} = \sqrt{\frac{\alpha_{11}N_V}{2k_{16}}} \quad (18)$$

The rate of every chain propagation step is equal, and this rate is also identical to the overall rate of the chain reaction:

$$-\frac{d[\text{O}_2]}{dt} = v_{11} = v_{11} = v_{11} = v_{11} \quad (19)$$

Combining eqs 15, 18, and 19 eliminates the steady-state concentration of the sulfate ion radical and gives the following rate equation:

$$-\frac{d[\text{O}_2]}{dt} = k_{15}\sqrt{\frac{\alpha_{11}}{2k_{16}}}[\text{Ce}^{3+}]N_V^{0.5} \quad (20)$$

This formula is in agreement with the experimentally found rate law given in eq 2 with

$$k_2 = k_{15} \times \alpha_{11}^{0.5} \times (2k_{16})^{-0.5} \quad (21)$$

According to the rate law for the termination step (eq 16), the concentration of the sulfate ion radical will fall to zero in the dark period following the usual second-order decay kinetics:

$$[\text{SO}_4^{\cdot-}] = \frac{[\text{SO}_4^{\cdot-}]_{\text{ss}}}{1 + 2k_{16}[\text{SO}_4^{\cdot-}]_{\text{ss}}t} \quad (22)$$

Comparing eqs 6 and 21 gives

$$k_6 = 2k_{16}[\text{SO}_4^{\cdot-}]_{\text{ss}} \quad (23)$$

In summary, the scheme given in reactions 11–16 provides coherent interpretation for all the experimental observations.

Further Mechanistic Points. It should be noted that the values of the rate constants k_{12} – k_{16} could not be determined directly from the measurements. However, it is possible to find estimates for the important rate constants using plausible chemical considerations.

It is clear that k_{16} is a second-order rate constant and cannot be larger than the diffusion controlled limit of $10^{10} \text{ M}^{-1} \text{ s}^{-1}$. In fact, the recombination rate constant of the sulfate ion radical was estimated in an earlier work⁵¹ to be

$$k_{16} = 4.4 \times 10^8 \text{ M}^{-1} \text{ s}^{-1} \quad (24)$$

Combining eqs 23 and 24 gives

$$[\text{SO}_4^{\cdot-}]_{\text{ss}} = 2.2 \times 10^{-9} \text{ M} \quad (25)$$

Combining eqs 17 and 23 gives a value for α_{11} :

$$\alpha_{11} = 0.15 \quad (26)$$

This is not an unreasonable quantum efficiency for reaction 11.⁴⁸

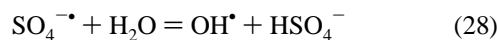
(49) Heidt, L. J.; McMillan, A. F. *Science* **1953**, *117*, 75.

(50) Espenson, J. H. *Chemical Kinetics and Reaction Mechanisms*, 2nd ed.; McGraw-Hill: New York, 1995; pp 181–189.

Finally, from eq 21 one can deduct

$$k_{15} = 2.3 \times 10^6 \text{ M}^{-1} \text{ s}^{-1} \quad (27)$$

It should be noted that the sulfate ion radical was reported to react with water in a reaction giving a hydroxyl radical and hydrogen sulfate ion with a first-order rate constant of 440 s^{-1} .⁵²



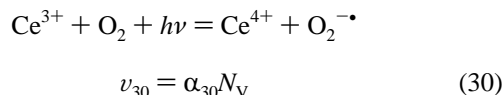
This reaction could in principle compete with reaction 15 under the concentration range of this study. However, it is also well-known that the sulfate ion radical can be favorably produced by the reaction of hydroxyl radical and hydrogen sulfate ion in sulfuric acid.⁵³ This is the exact reverse of reaction 30. Since sulfuric acid was used in the present study, the equilibrium of reaction 30 is probably shifted considerably to the left and thus the formation of the hydroxyl radical is not feasible.

One can also calculate the average chain length,⁵⁰ r , for the conditions used in the experiments with interrupted illumination:

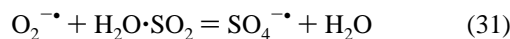
$$r = \frac{\nu_{15}}{\nu_{16}} = \frac{k_{15}[\text{Ce}^{3+}]}{k_{16}[\text{SO}_4^{\cdot-}]_{\text{ss}}} = 1.2 \times 10^3 \quad (29)$$

This expression also shows that the use of the long chain approximation is justified.⁵⁰

According to previous studies on the photochemistry of Ce^{3+} , it is possible that the leaving electron reacts with dissolved oxygen instead of water to form the superoxide ion in the primary photochemical process.⁴⁸



Consequently, the initiation sequence may proceed via alternative or parallel steps. Superoxide ion is expected to oxidize sulfite ion in a fast reaction:



Thus, the overall effect of the change in the initiation step is that one photon would start two chains and not one. In the limiting case, this would introduce a factor of 2 on the left side of eq 17 and subsequent expressions, but the derivation remains unaltered. Therefore, the main considerations are the same regardless of whether the real initiation occurs in a specific reaction or it is some sort of a linear combination of reactions 11 and 30.

As noted earlier, the reaction of $\text{SO}_5^{\cdot-}$ with Ce^{3+} was not considered in the final kinetic model primarily because it would have introduced branching into the chain, whereas the experimental data clearly indicate an unbranched chain reaction. Strictly speaking, this implies only that $\text{SO}_5^{\cdot-}$ reacts more favorably with $\text{H}_2\text{O} \cdot \text{SO}_2$ than with Ce^{3+} , which is usually present at somewhat lower concentration levels. At first sight, this finding is somewhat unexpected because $\text{SO}_5^{\cdot-}$ is known

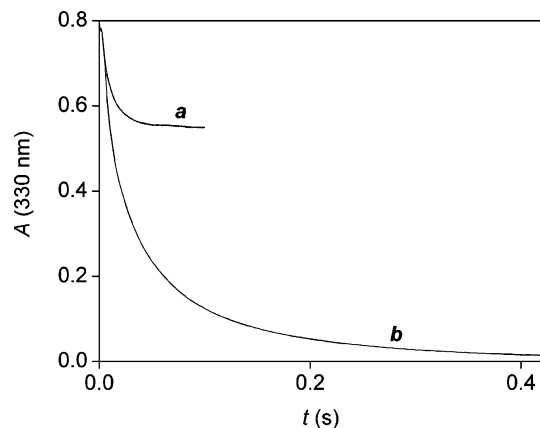


Figure 9. Kinetic traces measured in the reaction of sulfite ion and Ce^{4+} in the presence and absence of oxygen. $[\text{Ce}^{4+}] = 0.20 \text{ mM}$; $[\text{S(IV)}] = 0.20 \text{ mM}$; $[\text{O}_2] = 0.20 \text{ mM}$ (a), 0 (b); $[\text{H}_2\text{SO}_4] = 0.10 \text{ M}$; path length 1.000 cm ; $T = 25.0 \text{ }^\circ\text{C}$; $\lambda = 330 \text{ nm}$.

to react rapidly (with a second-order rate constants of about $10^8 \text{ M}^{-1} \text{ s}^{-1}$) with Fe^{2+} and Mn^{2+} ions.^{22,54} Appropriate kinetic data are not available for direct comparison of the oxidation rates of Ce^{3+} and the other metal ions. However, the thermodynamic driving force is considerably less for the oxidation of Ce^{3+} than for that of Fe^{2+} and Mn^{2+} . This difference predicts a much slower reaction with Ce^{3+} if the oxidation occurs in an outer-sphere complementary electron-transfer process. An additional reaction path through an initial oxygen transfer step followed by other processes can also be imagined in the oxidation of Fe^{2+} and Mn^{2+} which may exist in various higher oxidation states as oxo species. In contrast, such a reaction path is unlikely to be operative with Ce^{3+} and cannot enhance the oxidation rate.

Qualitative Tests for the Validity of the Mechanism. The mechanism proposed in the previous section has several verifiable implications. Some of these predictions were tested in this work.

The first prediction is that the oxidation of sulfite ion by Ce^{4+} , if carried out in the presence of dissolved oxygen, should consume O_2 as well. In other words, there must be some sort of synergy between the two oxidative processes. This was experimentally confirmed by three different methods. An experiment with the oxygen measuring probe was carried out where Ce^{4+} was added to an air-equilibrated acidic sulfite ion solutions (Figure S9). The loss in oxygen concentration was quite rapid. In another experiment, the oxidation of sulfite ion by Ce^{4+} was followed by measuring the absorbance decrease at 330 nm in a stopped-flow instrument (Figure 9). In the presence of dissolved oxygen, less Ce^{4+} was consumed than in the presence of oxygen clearly implying that O_2 rather than Ce^{4+} was the oxidizing agent for most of the sulfite ion present in the solution. The third method was also a stopped-flow experiment, but sulfite ion was used in small excess and the absorbance was followed at 276 nm (Figure S10). More sulfite ion was consumed when dissolved oxygen was present. All of these observations are consistent with the implications of the proposed model. These experiments also prove that the role of oxygen is not negligible in the analytical methods based on the Ce^{4+} –sulfite ion reaction.^{39–41}

(51) Huie, R. E.; Clifton, C. L. *Chem Phys. Lett.* **1993**, *205*, 163.

(52) Bao, Z. C.; Barker, J. R. *J. Phys. Chem.* **1996**, *100*, 9780.

(53) Neta, P.; Huie, R. E.; Ross, A. B. *J. Phys. Chem. Ref. Data* **1988**, *17*, 1027.

(54) Berglund, J.; Elding, L. I.; Buxton, G. V.; Salmon, G. A. *J. Chem. Soc., Faraday Trans.* **1994**, *90*, 3309.

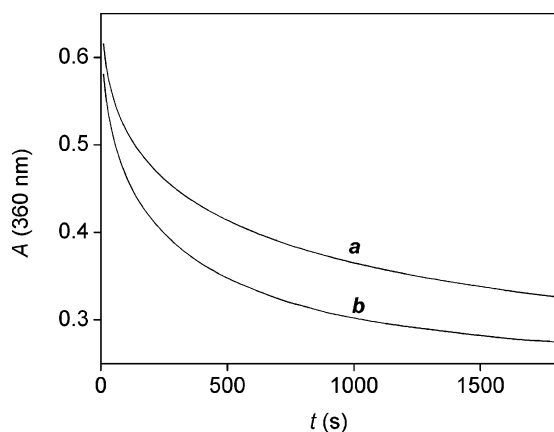


Figure 10. Kinetic traces measured in the sulfite ion–iron(III)–oxygen system in the presence and absence of Ce^{3+} . $[\text{Fe}^{3+}] = 2.0 \text{ mM}$; $[\text{S(IV)}] = 2.0 \text{ mM}$; $[\text{Ce}^{3+}] = 0$ (a), 0.20 mM (b); $[\text{H}_2\text{SO}_4] = 0.010 \text{ M}$; $[\text{O}_2] = 0.20 \text{ mM}$; path length 1.000 cm ; $T = 25.0 \text{ }^\circ\text{C}$; $\lambda = 360 \text{ nm}$.

Another important implication of the proposed model is that Ce^{3+} participates not only in photochemical initiation of the chain reaction, but also in maintaining it. In many earlier studies on catalytic autoxidation of sulfite ion, the postulated mechanisms involve the generation of sulfite ion radical in a chain reaction.^{3,5,22} Our kinetic model implies that Ce^{3+} has a cocatalytic or synergistic effect in these systems because it can increase the efficiency of the chains. This possible effect was experimentally confirmed in the extensively studied iron(III)–sulfite ion–oxygen system. A general feature of this system is that iron(III)–sulfite complex(es) form in the beginning of the reaction, the decomposition of which is dependent on the rate

of oxygen loss.^{22,37–38} Kinetic traces recorded in the presence and absence of Ce^{3+} are shown in Figure 10. This experiment was performed in a scanning spectrophotometer, where the only light going through the sample is the weak monochromatic (360 nm) analyzing beam, which is not absorbed by Ce^{3+} . The absorbing species at this wavelength are the iron(III)–sulfite complexes. It is clearly seen that the presence of Ce^{3+} accelerates the decomposition of the iron(III)–sulfite complexes and therefore the rate of autoxidation of sulfite ion, which is in agreement with the expectations based on the mechanism.

In conclusion, the results presented here clarify important aspects of the autoxidation of sulfite ion and may be crucial in exploring the detailed chemical background of the related analytical procedures. The synergistic effects demonstrated here offer the possibility of using Ce(III) as a cocatalyst in industrial oxidations of sulfur species. Furthermore, the experimental method and the mathematical treatment used in this paper for the particular example of the autoxidation of sulfite ion are also applicable to a much wider range of photoinitiated chain reactions.

Acknowledgment. This paper is dedicated to Prof. Ernő Brücher on his 70th birthday. The authors also thank the Hungarian Research Fund for financial support under Grant Numbers OTKA T042755 and M028244.

Supporting Information Available: A figure showing the spectra of Ce(III) and S(IV); nine figures demonstrating various kinetic effects in the title reaction. This material is available free of charge via the Internet at <http://pubs.acs.org>.

JA0439120